



Assessment of mitochondrial function following short- and long-term exposure of human bronchial epithelial cells to total particulate matter from a candidate modified-risk tobacco product and reference cigarettes



Dominika Malinska^a, Jędrzej Szymański^a, Paulina Patalas-Krawczyk^a, Bernadeta Michalska^a, Aleksandra Wojtala^a, Monika Prill^a, Małgorzata Partyka^a, Karolina Drabik^a, Jarosław Walczak^a, Alain Sewer^b, Stephanie Johnne^b, Karsta Luettich^b, Manuel C. Peitsch^b, Julia Hoeng^b, Jerzy Duszyński^a, Joanna Szczepanowska^{a,1}, Marco van der Toorn^{b,*,1}, Mariusz R. Wieckowski^{a,*,*,1}

^a Nencki Institute of Experimental Biology, Polish Academy of Sciences, 3 Pasteur Street, 02-093 Warsaw, Poland

^b PMI R&D, Philip Morris Products S.A., Quai Jeanrenaud 5, 2000 Neuchâtel, Switzerland

ARTICLE INFO

Keywords:

Mitochondria
Mitochondrial respiratory chain
Oxidative stress
BEAS-2B cells
Cigarette
Tobacco heating system

ABSTRACT

Mitochondrial dysfunction caused by cigarette smoke is involved in the oxidative stress-induced pathology of airway diseases. Reducing the levels of harmful and potentially harmful constituents by heating rather than combusting tobacco may reduce mitochondrial changes that contribute to oxidative stress and cell damage. We evaluated mitochondrial function and oxidative stress in human bronchial epithelial cells (BEAS 2B) following 1- and 12-week exposures to total particulate matter (TPM) from the aerosol of a candidate modified-risk tobacco product, the Tobacco Heating System 2.2 (THS2.2), in comparison with TPM from the 3R4F reference cigarette. After 1-week exposure, 3R4F TPM had a strong inhibitory effect on mitochondrial basal and maximal oxygen consumption rates compared to TPM from THS2.2. Alterations in oxidative phosphorylation were accompanied by increased mitochondrial superoxide levels and increased levels of oxidatively damaged proteins in cells exposed to 7.5 µg/mL of 3R4F TPM or 150 µg/mL of THS2.2 TPM, while cytosolic levels of reactive oxygen species were not affected. In contrast, the 12-week exposure indicated adaptation of BEAS-2B cells to long-term stress. Together, the findings indicate that 3R4F TPM had a stronger effect on oxidative phosphorylation, gene expression and proteins involved in oxidative stress than TPM from the candidate modified-risk tobacco product THS2.2.

1. Introduction

Oxidative stress caused by tobacco smoke can result in inflammation, epithelial injury, and cell death, and is a major causative factor in airway diseases such as chronic obstructive pulmonary disease and lung cancer (Durham and Adcock, 2015; Rahman and MacNee, 1996). Because tobacco smoke contains thousands of harmful and potentially harmful constituents (HPHCs) such as radicals, carcinogens, aromatic hydrocarbons, and α , β -unsaturated aldehydes (Baker, 1974; Rodgman and Perfetti, 2013), it is likely that the toxicity associated with oxidative stress is the result of a complex interaction of a variety of constituents, reacting either directly or indirectly with the extracellular and

intracellular components of the respiratory tract.

Mitochondria are among the first responders to various stress factors that challenge cell and tissue homeostasis. Therefore, mitochondrial malfunction is increasingly recognized as a key component in acute and chronic cellular stress. *In vitro* and *in vivo* studies have shown that HPHCs in tobacco smoke can disturb the complexes of the mitochondrial respiratory chain (Anbarasi et al., 2005; van der Toorn et al., 2007). When this happens, a proton motive force across the inner mitochondrial membrane cannot be generated, leading to mitochondrial respiratory chain inhibition, and electrons leak from the electron transfer chain and react with oxygen to form reactive oxygen species (ROS) (Lebiedzinska et al., 2013; van der Toorn et al., 2009; Wojewoda

* Corresponding author. Systems Toxicology, Biological Systems Research, Philip Morris International, R&D, Switzerland.

** Corresponding author. Laboratory of Bioenergetics and Biomembranes, Department of Biochemistry, Nencki Institute of Experimental Biology, Polish Academy of Sciences, Poland.

E-mail addresses: Marco.vanderToorn@pmi.com (M. van der Toorn), m.wieckowski@nencki.gov.pl (M.R. Wieckowski).

¹ These three authors share senior co-authorship.

Abbreviations

A.U.	Arbitrary units
CS	Cigarette smoke
COPD	Chronic obstructive pulmonary disease
cyt.ROS	Cytosolic reactive oxygen species
DMSO	Dimethyl sulfoxide
ECAR	Extracellular acidification rate
EDTA	Ethylenediaminetetraacetic acid

FCCP	Carbonyl cyanide-4-(trifluoromethoxy)phenylhydrazone
HPHCs	Harmful and potentially harmful constituents
mtO ₂ ^{•−}	Mitochondrial superoxide
OCR	Oxygen consumption rate
Rpm	Rounds per minute
ROS	Reactive oxygen species
THS	Tobacco heating system
TPM	Total particulate matter

et al., 2010, 2011). Apart from increased generation, elevated ROS levels also depend on the levels of antioxidant enzymes, which form the first line of defense against ROS. Furthermore, impaired mitochondrial functions not only affect energy production and ROS levels, but also exert a significant impact on cellular physiology. The consequences of mitochondrial malfunction in lung epithelium are reflected in significant changes in epithelial barrier function, inflammation, and lung injury, which are seen in patients with tobacco smoke-induced lung diseases (CDC, 2010).

Lowering HPHC levels by heating rather than combusting tobacco is a promising approach in reducing mitochondrial dysfunction and cellular stress associated with smoking combustible tobacco products. Heating rather than combusting tobacco has been shown to substantially reduce HPHC levels in the resulting aerosol (Patskan and Reininghaus, 2003). In a 90-day nose-only inhalation study in Sprague–Dawley rats, it was demonstrated that exposure to aerosol from a new candidate modified-risk tobacco product (cMRTP), the Tobacco Heating System 2.2 (THS2.2), significantly reduced the degree of cellular stress and lung inflammation compared with exposure to tobacco smoke from the 3R4F reference cigarette (Wong et al., 2016). In the present study, we evaluated the mitochondrial function of cultured human bronchial epithelial cells following short- and long-term exposure to total particulate matter (TPM) from THS2.2 aerosol and 3R4F cigarette smoke (CS).

THS2.2 is a battery-operated heating system into which a tobacco stick is inserted and heated at a maximum temperature of 350 °C; this generates an aerosol primarily composed of water, glycerol, and nicotine (Smith et al., 2016). In contrast, during the combustion of conventional cigarettes, the temperature of the tobacco increases up to 900 °C, resulting in more than 6000 combustion and pyrolysis products (Baker, 1974; Rodgman and Perfetti, 2013). TPM, which represents the particulate phase of mainstream tobacco smoke, comprises approximately 80% of the total weight of tobacco smoke (Barsanti et al., 2007). We used TPM as the test item to investigate the effects of HPHCs, as multiple HPHCs have been found in TPM (Rodgman and Perfetti, 2013).

To assess mitochondrial physiology, a human immortalized bronchial epithelial cell line, BEAS-2B, was continuously exposed to TPM from 3R4F CS and three different concentrations of TPM from THS2.2 aerosol for 1 or 12 weeks. Multiple cellular parameters were measured, including mitochondrial oxygen consumption, ROS levels, the efficiency of the antioxidant defense system, and markers of oxidative stress. This enabled us to assess the impact of the THS2.2 TPM on mitochondrial functions in bronchial epithelial cells in comparison with those seen following exposure to CS TPM.

2. Materials and methods

2.1. Chemicals

MitoSOXTM Red (mitochondrial superoxide indicator), CM-H₂DCFDA (general oxidative stress indicator), and JC-1 (mitochondrial membrane potential probe) were obtained from Invitrogen (Carlsbad, CA, USA). Total OXPHOS rodent antibody cocktail and anti-SOD2 antibody were obtained from Abcam (Cambridge, UK). Antibody against

GPx1 was obtained from Cell Signaling Technology (Danvers, MA, USA). Antibody against GAPDH was obtained from Merck Millipore (Billerica, MA, USA). Antibody against SOD1 was obtained from Santa Cruz Biotechnology (Dallas, TX, USA). CellTiter-Glo[®] 2.0 was obtained from Promega (Madison, WI, USA). Anti-rabbit IRDye 800CW antibody were obtained from LI-COR Biosciences (Lincoln, NE, USA). Antibody against anti-β-actin, DMSO, ATP, pyruvate, oligomycin, carbonyl cyanide-4-(trifluoromethoxy)phenylhydrazone (FCCP), mercaptoethanol, glycerol, HCl, Tween[®] 20, glucose, H₂O₂, Tris and antimycin A were obtained from Sigma-Aldrich (St. Louis, MO, USA). Glutamine was obtained from GE Healthcare Bio-Sciences (Pittsburgh, USA).

2.2. Cell culture

The human bronchial epithelial cell line BEAS-2B was obtained from the American Type Culture Collection (ATCC, #CRL-9609; Manassa, VA, USA). Cells were cultured in bronchial epithelial cell growth medium consisting of bronchial epithelial cell basal medium supplemented with a SingleQuots[™] kit (Lonza Walkersville, MD, USA), following the vendor's recommendations. Cells were grown in 75-cm² collagen I-coated culture flasks (VWR, Radnor, PA, USA) at 37 °C in an atmosphere of 5% CO₂ until reaching 75%–80% confluence. A TC20 Automated Cell Counter and Muse Count & Viability Assay (Bio-Rad Laboratories, Hercules, CA, USA) were used to count the cells and assess cell viability according to the manufacturer's instructions. Substances were added to cells 4 h after seeding on culture dishes.

2.3. Generation of 3R4F and THS2.2 TPM

3R4F reference cigarettes were purchased from the University of Kentucky (Lexington, KY, USA; <http://www.ca.uky.edu/refcig/>). THS2.2 sticks and stick holders were provided by Philip Morris Products S.A. (Neuchâtel, Switzerland); the holder heats the tobacco plug to generate an aerosol containing water, glycerin, nicotine, and tobacco flavors (Smith et al., 2016). The tobacco stick holder includes a battery, electronics for control, a heating element, and a stick extractor. Prior to use, 3R4F cigarettes and THS2.2 sticks were conditioned according to ISO Standard 3402 (International Organization for Standardization, 2010) for at least 48 h at a temperature of 22 ± 1 °C and a relative humidity of 60 ± 3% before being used for smoke or aerosol generation. Smoke from 3R4F cigarettes was generated on a 20-port Borgwaldt smoking machine (Hamburg, Germany), and aerosol from THS2.2 was generated on a 30-port SM2000/P1 smoking machine (Philip Morris International, Neuchâtel, Switzerland) according to the Health Canada Intense protocol (55 mL puff volume; 2-s puff duration; 2 min^{−1} puff frequency; 100% blocking of 3R4F filter ventilation holes) (Health Canada, 1999). TPM from the mainstream smoke of 3R4F reference cigarettes or aerosol from THS2.2 sticks was trapped on glass fiber filters, from which it was then extracted with an appropriate volume of DMSO to give a final concentration of 100 mg TPM/mL.

2.4. TPM exposure

The assessment of mitochondrial function was performed using

BEAS-2B cells collected during the long-term exposure study described by van der Toorn et al. (van der Toorn et al., 2018). In brief, BEAS-2B cells were exposed to TPM from 3R4F (7.5 µg/mL) or low, medium, and high concentrations of TPM from THS2.2 aerosol (7.5, 37.5, or 150 µg/mL, respectively) for either 1 or 12 weeks in cell culture flasks. Cells in medium with 0.1% (v/v) DMSO were included as a vehicle control.

2.5. Measurement of ATP levels

BEAS-2B cells were evenly seeded on 96-well collagen I-coated white plates (Corning BioCoat, Corning, NY, USA). ATP levels were measured using a CellTiter-Glo[®] 2.0 assay in an Infinity microplate reader (Tecan, Männedorf, Switzerland), according to the manufacturer's instructions. A standard curve was prepared to calculate cellular ATP content, according to the kit manual. ATP measurements were normalized to the mean cell count in each particular exposure group.

2.6. Measurement of oxygen consumption

The mitochondrial oxygen consumption rate (OCR) in intact cells was measured with a Clark electrode (5300A biological oxygen monitor; YSI, Rye Brook, NY, USA). All measurements were performed at 37 °C. Cells growing on 75-cm² culture flasks were harvested with Accutase (Gibco, Waltham, MA, USA), rinsed with ice-cold phosphate-buffered saline (PBS), and sedimented by centrifugation. Cells were then resuspended in PBS containing Ca²⁺ and Mg²⁺ ions; the total number of cells and the number of living cells were estimated with an automated cell counter and cell viability assay, respectively. The cell suspension was transferred to a measurement chamber, where the basal respiration rate was recorded in the presence of 5 mM pyruvate. Next, 1 µM oligomycin was added to inhibit oxygen consumption related to ATP synthesis and to measure proton leak. To measure uncoupled (maximal) respiration rate, 0.5 µM FCCP was added. Respiration driving ATP production under basal conditions (basal respiration rate minus proton leak), the coupling efficiency (basal respiration rate divided by basal respiration), and the spare respiratory capacity (maximal respiration rate minus basal respiration rate) were calculated.

2.7. Seahorse phenotype test

The extracellular acidification rate (ECAR) and OCR of cells at starting assay conditions and under energy demand were measured using the Seahorse XF96 Extracellular Flux Analyzer (Seahorse Bioscience, North Billerica, MA, USA) according to the manufacturer's instructions. Briefly, Seahorse XFp DMEM media (Seahorse) supplemented with 1 mM pyruvate, 2 mM glutamine, and 10 mM glucose was used. Oligomycin (final concentration: 1 µM) and FCCP (final concentration: 1.5 µM) were simultaneously applied to measure the two major energy-producing pathways in the cells.

2.8. Whole-cell extracts and immunoblotting

Cells growing on 75-cm² culture flasks were harvested with Accutase[®] (Gibco), rinsed with ice-cold PBS, sedimented by centrifugation, resuspended in RIPA lysis buffer (Sigma-Aldrich) with protease and phosphatase inhibitor cocktails (Sigma-Aldrich), and incubated for 20 min on ice. Next, cell lysates were centrifuged at 16,000 × g for 20 min at 4 °C to remove insoluble cellular material. The supernatants were collected and protein concentration was determined according to the Bradford method (Bradford, 1976). The samples were supplemented with reducing Laemmli loading buffer (0.5 M Tris-HCl, 2.3% SDS, 5% mercaptoethanol [v/v], 12.5% glycerol [v/v]; pH 6.8) and denatured at 95 °C or 45 °C (in the case of OXPHOS subunits detection) for 5 min. Lysates containing equal amounts of protein (10–50 µg) were separated by SDS-PAGE, transferred to nitrocellulose or PVDF membranes, and blocked in Odyssey Blocking Buffer (LI-COR

Biosciences) diluted 1:1 in Tris-buffered saline for 1 h. Blots were then incubated overnight with primary antibodies at appropriate concentrations (as described in the following section), rinsed with PBS-0.1% Tween 20, and incubated with fluorescently labeled secondary antibodies for 1 h in a 1:10,000 dilution.

To evaluate the levels of proteins of interest, the following primary antibodies were used: Total OXPHOS rodent antibodies cocktail (1:1000), anti-GPx1 (1:1000); anti-GAPDH (1:20,000), anti-SOD2 (1:1000), anti-SOD1 antibody (1:1000) and anti-β-actin antibody (1:150,000).

The relative levels of the proteins on the membranes were visualized using an Odyssey Infrared Imaging System (LI-COR Biosciences). The fluorescence intensity of the bands was analyzed using Image Studio[™] software for the Odyssey[®] 3021. Protein level was expressed relatively to β-actin or GAPDH as a reference protein.

2.9. Measurement of cytosolic ROS levels

Three days before the end of the TPM exposure, cells were seeded in 24-well plates at a density of 3500–7000 cells per well. Seeding density was individually adjusted for each exposure group to account for differences in proliferation intensities, so that on the day of the measurement, all cells had similar confluence (about 80%). On the day of measurement, cells were treated for 30 min at 37 °C with 1 µM CM-H₂DCFDA ROS indicator in PBS containing 5.56 mM glucose. Next, cells were rinsed twice with fresh PBS, and 0.5 mL of fresh glucose-supplemented PBS were added to each well. Cytosolic ROS levels were measured with an iCys laser scanning cytometer (20 × objective; Thorlabs, Newton, NJ, USA). From each well, 9–12 fields of view were collected and analyzed. A single field of view corresponded to an image size of 500 × 384. The fluorescence intensity of the oxidized probe was measured at λ_{Ex} = 488 nm and λ_{Em} = 530 nm, using a 530/30 nm filter cube. As a positive control, cells were loaded in the presence of 20 µM H₂O₂. For probe-loading, washing, and measurements, PBS containing 0.9 mM CaCl₂ and 0.49 mM MgCl₂ was used. Images were analyzed with the iCys software (Thorlabs). Each microscopy image was divided into smaller regions (phantom contours) in which the fluorescent signal was quantified. Based on the histogram of the obtained phantom intensities, different areas of the image corresponding to the signal and background were identified. The radius of the applied phantom contours was in the range of 1–2 µm. The mean number of detected phantom contours per well was in the order of 10⁴–10⁵, corresponding to several hundred (10²–10³) cells. The signal originating from the cells at the edge of the image was discarded, and only the signal from singly illuminated 2', 7'-dichlorofluorescein (DCF) was integrated over the whole cell. The cells situated at the edge of the field of view were illuminated several times during image acquisition of neighboring areas, resulting in a strong signal increase in those areas owing to the photo-activation of the DCF probe.

2.10. Measurement of mitochondrial superoxide (mt.O₂⁻) levels

Cells were exposed and seeded in 24-well plates in the same manner as for cytosolic ROS measurements (Section 2.9). On the day of measurement, cells were treated for 30 min at 37 °C with 5 µM mitochondrial superoxide indicator MitoSOX[™] Red in PBS containing 5.56 mM glucose. Next, cells were rinsed twice with fresh PBS, and 0.5 mL of fresh glucose-supplemented PBS was added to each well. Levels of mitochondrial superoxide were measured with an iCys laser scanning cytometer (20 × objective). The fluorescence intensity of the oxidized MitoSOX[™] Red was measured at λ_{Ex} = 488 nm and λ_{Em} = 580 nm. As a positive control, 1 µg/µL antimycin A was added to the selected wells. For probe-loading, washing, and measurements, PBS containing 0.9 mM CaCl₂ and 0.49 mM MgCl₂ was used. As in the case of cytosolic ROS measurement, collected images were analyzed using the iCys software while applying the phantom contour method. Only the cytosolic signal

of oxidized MitoSOX™ Red was analyzed.

2.11. Detection of oxidatively modified proteins

The levels of carbonylated proteins were estimated using an OxyBlot Protein Oxidation Detection Kit (Merck Millipore). Protein aliquots (7.5 µg) were prepared according to the manufacturer's protocol and separated on 10% SDS-PAGE. The dinitrophenyl (DNP)-derivatized proteins were detected by incubation with rabbit anti-DNP antibody (1:150) followed by incubation with anti-rabbit IRDye® 800CW antibody (1:5000; LI-COR Biosciences), both in Odyssey Blocking Buffer (LI-COR Biosciences). Levels of oxidatively modified proteins were normalized to GAPDH levels.

2.12. Generation and analysis of transcriptomics data

The material used in this study corresponds to a subset of the BEAS-2B cells collected during the long-term exposure study described by van der Toorn et al. (van der Toorn et al., 2018). Therefore, the transcriptomics data were readily obtained by extracting the 1- and 12-week values from the corresponding ArrayExpress submission (E-MTAB-5697), disregarding the 2-, 4-, and 8-week exposure groups. We focused on a subset of genes related to the oxidative stress response, which was obtained by intersecting the microarray gene annotation and

the 84 genes contained in the biologically relevant “Human Oxidative Stress QIAseq Targeted RNA Virtual” panel (<https://www.qiagen.com/ch/shop/sequencing/qiaseq-targeted-rna-virtual-panels/?catno=CRHS-00065Z-100#geneglobe>). The corresponding gene response to the exposures was quantified by applying the moderated statistics-based approach implemented in the Limma R package to eight pairwise comparisons between the four TPM-exposed groups (3R4F TPM, and low-, medium-, and high-dose THS2.2 TPM) and the matching DMSO-exposed control groups (Smyth, 2005). Linear models containing the biological replicate number as a covariate were used to estimate the differential expression, and raw p-values were calculated for each gene. The Benjamini-Hochberg false discovery rate (FDR) method was then applied to adjust the raw p-values for multiple testing effects (Benjamini and Hochberg, 1995). FDR values below 0.05 were considered statistically significant.

2.13. Statistical analysis

Statistical analysis of the data was performed in GraphPad Prism 6.0 (GraphPad Software, Inc., La Jolla, CA, USA). Principal component analysis (PCA) was performed in R.

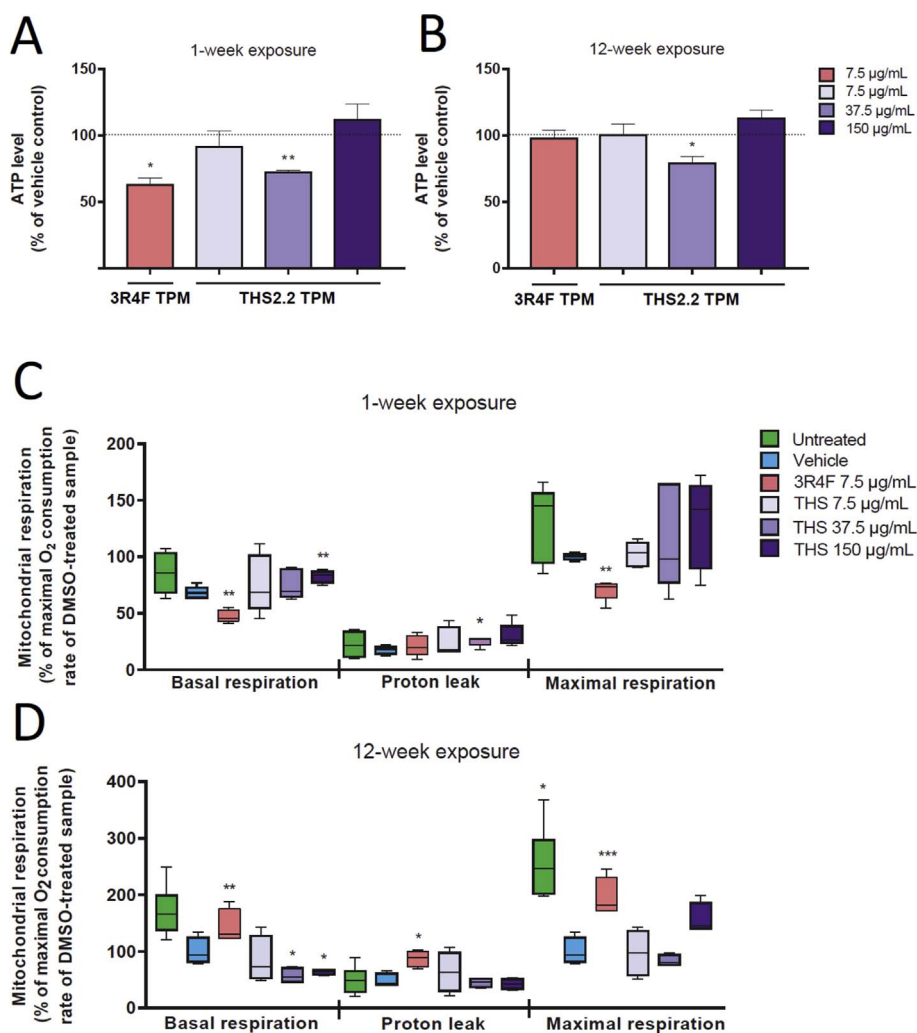


Fig. 1. Effects of total particulate matter (TPM) from 3R4F reference cigarette smoke (7.5 µg/mL) and THS2.2 aerosol (7.5, 37.5, and 150 µg/mL) on (A, B) cellular ATP levels and (C, D) basal respiration, proton leak, and maximal respiration in BEAS-2B cells. Cells were exposed for 1 week (A, C) or 12 weeks (B, D). Data shown are means ± SEM. *p < 0.05, **p < 0.01, ***p < 0.001 versus vehicle (DMSO)-exposed cells. ATP levels: n = 3 for 1-week exposure; n = 4 for 12-week exposure versus vehicle (DMSO)-exposed cells. Mitochondrial respiration: n = 5 for 1-week exposure; n = 4 for 12-week exposure versus vehicle (DMSO)-exposed cells.

3. Results

3.1. TPM from 3R4F cigarette smoke and from THS2.2 aerosol decreases ATP levels in the BEAS-2B cells dependent on exposure time and dose

To elucidate the effect of short and chronic exposure to TPM from 3R4F CS and TPM from THS2.2 aerosol on cellular bioenergetics of human bronchial epithelial BEAS-2B cells, we examined the ATP levels in response to exposure. Changes in the ATP level can suggest mitochondrial defect and can highlight alterations in cellular energy production processes. One-week exposure to 7.5 µg/mL of 3R4F TPM significantly decreased the level of ATP in BEAS-2B cells versus vehicle

(DMSO)-exposed cells (Fig. 1A). However, 3R4F TPM had no effect on ATP levels in cells exposed for 12 weeks (Fig. 1B). Similarly, the low and high concentrations of TPM from THS2.2 aerosol (7.5 and 150 µg/mL) had no impact on BEAS-2B ATP levels, both after 1 and 12 weeks of exposure (Fig. 1A and B). Only the medium concentration of THS2.2 TPM (37.5 µg/mL) significantly decreased ATP levels after 1 week as well as after 12 weeks of exposure. These results clearly indicate metabolic alterations in cells exposed for 1 week to 3R4F TPM and in cells exposed to a medium concentration of THS2.2 TPM for 1 and 12 weeks. The effect of DMSO (DMSO vs. non-exposed cells) on ATP levels in BEAS-2B cells is shown in Supplementary Fig. 1. Interestingly, at both time points, DMSO-exposed cells had higher ATP levels than non-

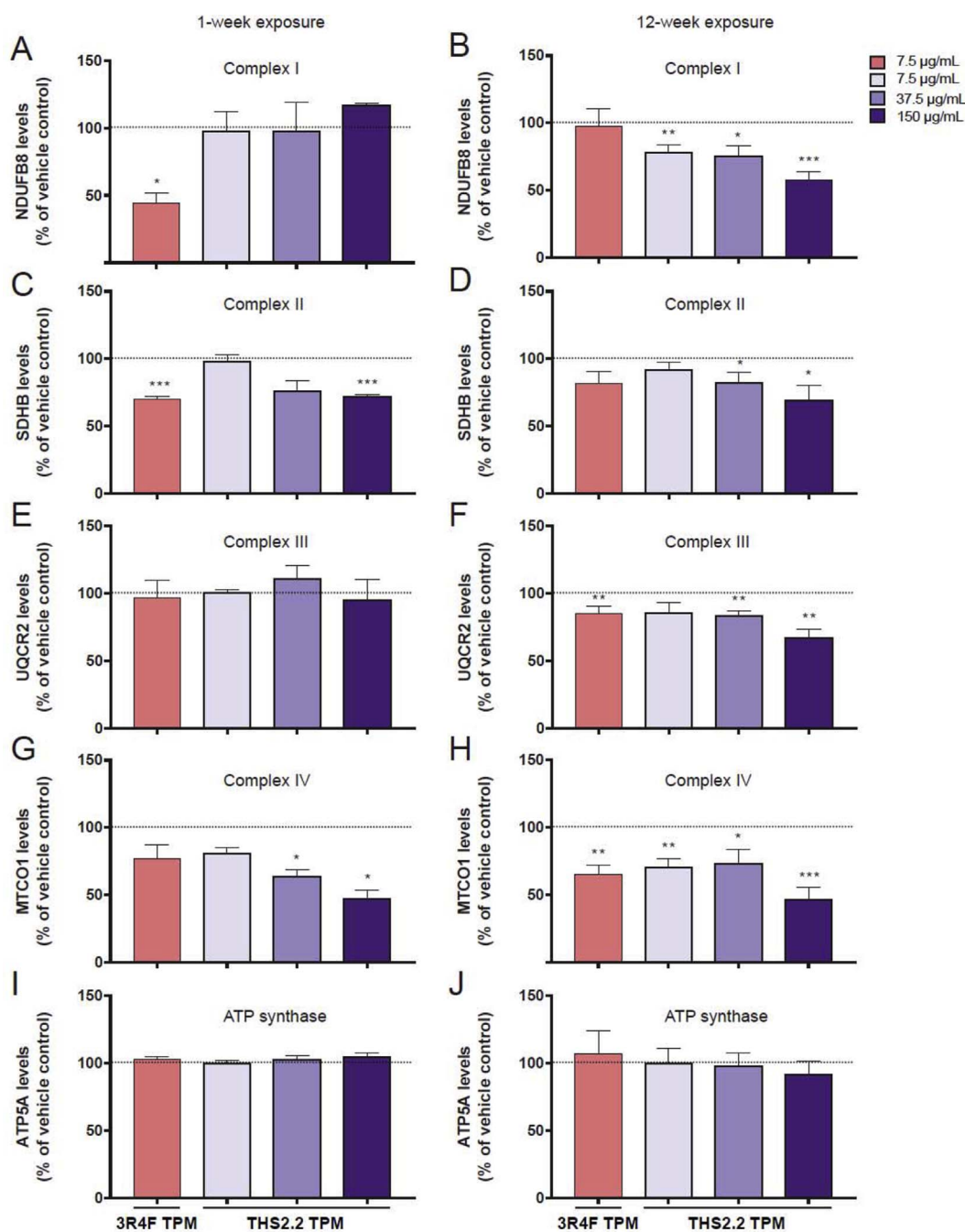


Fig. 2. Effects of 1- and 12-week exposures of BEAS-2B cells to total particulate matter (TPM) from 3R4F reference cigarette smoke (7.5 µg/mL) and THS2.2 aerosol (7.5, 37.5, and 150 µg/mL) on the levels of representative subunits of the mitochondrial respiratory chain complexes. Densitometry analysis of the representative subunits of oxidative phosphorylation markers (A, B) NDUFB8, (C, D) SDHB, (E, F) UQCQR2, (G, H) MTCO1, and (I, J) ATP5A. The levels of individual proteins were calculated as a ratio to β -actin. Data shown are means \pm SEM. * $p < 0.05$, ** $p < 0.01$, *** $p < 0.001$ of three (for NDUFB8) and four (for SDHB, UQCQR2, MTCO1 and ATP5A) independent experiments versus vehicle (DMSO)-exposed cells.

exposed BEAS-2B cells.

3.2. The effect of short- and long-term exposure to TPM from 3R4F cigarette smoke and from THS2.2 aerosol on mitochondrial respiration

To explore the possible mechanism by which TPM exposure affects ATP levels, we measured cellular oxygen consumption, which is related to mitochondrial respiratory chain function. The rate of respiration recorded at the initial phase of measurement corresponding to “Basal respiration” gives insights into the resting energetics of the cells. Addition of oligomycin inhibits mitochondrial ATP synthesis, which results in slowing the rate of oxygen consumption by the mitochondrial respiratory chain. The remaining oxygen consumption rate is used to compensate mitochondrial “Proton leak”, but can also have a non-mitochondrial origin (other cellular processes that use oxygen). In our studies, examination of non-mitochondrial respiration was omitted due to its negligible value. Next, addition of FCCP stimulates oxygen consumption to its maximum value (“Maximal respiration”) and shows the maximum capacity of the mitochondrial respiratory chain. Based on “Basal respiration”, “Proton leak” and “Maximal respiration”, it is possible to calculate parameters describing: a) the respiration rate being used to drive “ATP synthesis” under basal conditions, b) “Coupling efficiency” describing which fraction of “Basal respiration” is used to drive ATP production versus “Proton leak”, and c) “Spare Respiratory Capacity” indicating how close to maximal efficiency of the respiratory chain the cells are operating under basal conditions. As shown in Fig. 1C, 1-week exposure to 3R4F TPM decreased, while 1-week exposure to the highest dose of THS2.2 TPM (150 µg/mL) increased “Basal respiration” of BEAS-2B cells in comparison with vehicle-exposed controls. There were no significant changes in the “Proton leak” - coupled respiration in BEAS-2B cells exposed for 1 week to either 3R4F TPM or the lowest dose of TPM from THS2.2 aerosol. Only in cells incubated in medium or exposed to the highest dose of THS2.2 TPM (37.5 and 150 µg/mL) a higher proton leak was observed, suggesting that these exposures had a negative effect on the inner mitochondrial membrane. Additionally, there was a clear inhibitory effect of TPM from 3R4F CS on mitochondrial respiratory chain as evidenced by a ca. 25% decrease in “Maximal respiration” when compared with vehicle-exposed controls (Fig. 1C).

A slightly opposite effect is observed when TPM exposures are extended to 12 weeks (Fig. 1D). “Basal respiration” of cells exposed to TPM from 3R4F reference CS increased compared with vehicle controls. Moreover, increased “Proton leak” suggests a harmful effect of prolonged exposure to 3R4F TPM on the permeability of the inner mitochondrial membrane in BEAS-2B cells. In contrast, exposure of BEAS-

2B cells to medium or high doses of TPM (37.5 and 150 µg/mL) from THS2.2 aerosol decreased “Basal respiration”, suggesting these exposures had a negative effect on the mitochondrial respiratory chain (Fig. 1D). Interestingly, “Maximal respiration” following addition of FCCP to cells exposed to vehicle (DMSO) for 12 weeks was not higher than that seen in DMSO controls following 1 week of exposure, but similar to the value of “Basal respiration”. This indicates that long-term exposure to DMSO causes dysfunction of the mitochondrial respiratory chain. Moreover, comparison of the “Basal respiration” and “Maximal respiration” rates in vehicle (DMSO)-exposed cells and non-exposed cells clearly showed that 12-week exposure to DMSO has a strong inhibitory effect on the mitochondrial respiratory chain.

As mentioned above, based on the Basal and Maximal respiration rates and “proton leak”, we calculated additional parameters indicative of OXPHOS function. Results presenting oxygen consumption coupled to “ATP synthesis”, “Spare Respiratory Capacity” and “Coupling efficiency” calculated for individual exposures after 1 and 12 weeks are shown in Supplementary Fig. 2 A, C, E and Supplementary Fig. 2 B, D, F, respectively. The differences in the effects on respiration of BEAS-2B cells between 1- and 12-week exposure are clearly visible in oxygen consumption coupled to “ATP synthesis” and coupling efficiency.

3.3. The effect of short- and long-term exposure to TPM from 3R4F cigarette smoke and from THS2.2 aerosol on the expression levels of individual subunits of the mitochondrial respiratory chain and ATP synthase

To understand the effect of TPM exposure on oxygen consumption and to determine whether alterations in the oxygen consumption can be related to the changes in OXPHOS composition, we evaluated the expression level of individual subunits of the mitochondrial respiratory chain. With the use of antibodies against representative OXPHOS subunits (NDUFB8 - complex I, SDHB - complex II, UQCRC2 - complex III, MTCO1 - complex IV and ATP5A - ATP synthase) we evaluated the level of mitochondrial respiratory chain complexes I, II, III, IV and ATP synthase in BEAS-2B cells exposed to TPM from 3R4F CS and from THS2.2 aerosol for 1 or 12 weeks (Fig. 2). One-week exposure of BEAS-2B cells to 3R4F TPM caused a significant decrease in Complex I and II (Fig. 2A and C). The level of Complex IV also seemed to be decreased; however, the effect was not statistically significant (Fig. 2G). When BEAS-2B cells were exposed to THS2.2 TPM, there was a dose-dependent decrease in Complex II and IV levels. Prolonged exposure to 3R4F TPM caused a statistically significant decrease in the level of complexes III and IV (Fig. 2F and H). A dose-dependent effect on the level of all four respiratory chain complexes (I, II, III and IV) was observed for THS2.2 TPM exposures (Fig. 2B, D, F, and H). However, there was no

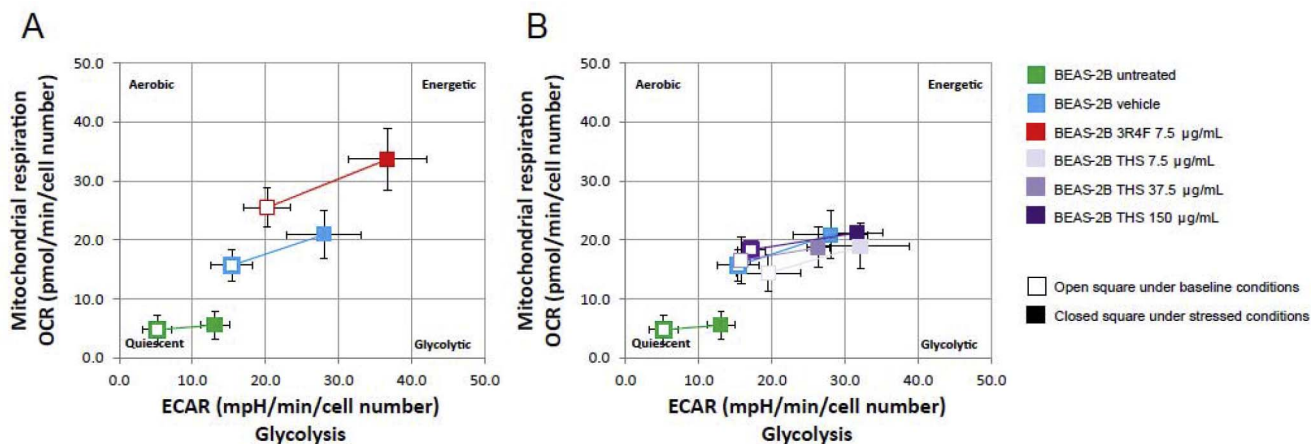


Fig. 3. Normalized metabolic phenograph of BEAS-2B cells exposed for 12 weeks to total particulate matter (TPM) from 3R4F reference cigarette smoke (A) and THS2.2 aerosol (B). The baseline phenograph shows differences in both glycolysis (extracellular acidification rate, ECAR) and mitochondrial respiration (oxygen consumption rate, OCR). The quadrants were set at arbitrary values to indicate only the direction of bioenergetic changes.

TPM exposure effect on the level of ATP synthase (Fig. 2I and J). Interestingly, 1-week exposure of BEAS-2B cells to vehicle (DMSO) increased the level of complex II, while 12-week exposure induced significant higher levels of complexes I, II, III and IV in comparison with the non-exposed BEAS-2B cells (data not shown).

3.4. Long-term exposure to TPM from 3R4F cigarette smoke and THS2.2 aerosol alters the metabolic phenotype of BEAS-2B cells

In order to examine if long term exposure-dependent differences in the profile of OXPHOS function parameters are connected with metabolic reprogramming, we measured the metabolic potential of BEAS-2B cells after 12 weeks of exposure to TPM (Fig. 3). The extracellular acidification rate (ECAR), which estimates glycolytic activity under certain conditions, and the mitochondrial oxygen consumption rate (OCR), which is a performance indicator of mitochondrial function, where both determined simultaneously within the BEAS-2B cell population. Twelve week exposure to TPM from 3R4F CS elevated both ECAR and OCR, indicating that the cells increased their metabolism due to increased glycolysis and mitochondrial function. This shifted the baseline phenotype of the original BEAS-2B cells from a quiescent to a more energetic phenotype compared with non-exposed or vehicle-exposed cells. This shift is known in oncology as the Warburg effect, and is thought to be an adaptation mechanism for supporting the biosynthetic requirements of uncontrolled proliferation (Liberti and Locasale, 2016). Long-term exposure of BEAS-2B cells to low, medium, and high concentrations (7.5, 37.5 and 150 $\mu\text{g}/\text{mL}$) of TPM from THS2.2 aerosol did not alter the metabolic phenotype compared with effects in the vehicle control (Fig. 3A and B).

3.5. The effect of short- and long-term exposure to TPM from 3R4F cigarette smoke and from THS2.2 aerosol on the oxidative stress manifestation in BEAS-2B cells

Alterations in mitochondrial function and especially dysfunction of the mitochondrial respiratory chain are very often accompanied by increased ROS production/level. Taking into account the effect of TPM exposures on mitochondrial oxygen consumption and on the level of

individual mitochondrial respiratory chain subunits, we investigated whether this translated into higher ROS levels or ROS production which may have detrimental consequences for the cells. First, we investigated global cytosolic ROS levels using a CM-H₂DCFDA probe. Interestingly, cytosolic ROS levels were not statistically significantly different in BEAS-2B cells exposed to 3R4F TPM or TPM from THS2.2 aerosol in comparison with vehicle-exposed cells, independent of the exposure period (Fig. 4A and B). On the other hand, mitochondrial superoxide level (mt.O₂^{•-}) measured with the use of MitoSOXTM Red probe, was found to be exclusively increased in cells exposed to TPM for 1 week (Fig. 4C), with an apparent dose-dependent effect of TPM from THS2.2 aerosol. In cells exposed to 3R4F TPM or to the highest dose of THS2.2 TPM (150 $\mu\text{g}/\text{mL}$), inhibition of electron transfer at respiratory complex III by antimycin A had no effect on the detected mt.O₂^{•-} levels, while the presence of this inhibitor in BEAS-2B cells exposed to lower THS2.2 TPM concentrations (7.5 and 37.5 $\mu\text{g}/\text{mL}$) increased mt.O₂^{•-} to the levels observed in 3R4F TPM-exposed cells (data not shown). This suggests that the observed mt.O₂^{•-} increase is caused by enhanced ROS production by the respiratory chain. In contrast, in cells exposed for 12 weeks, the level of mt.O₂^{•-} was unchanged (Fig. 4D). In fact, there was even a small decrease in the level of this free radical in BEAS-2B cells exposed to the low dose of THS2.2 TPM (7.5 $\mu\text{g}/\text{mL}$) for 12 weeks (Fig. 4B).

In short-term 3R4F TPM-exposed cells higher mt.O₂^{•-} levels correlated with increased levels of carbonylated proteins, indicating oxidative stress in these cells (Fig. 4E and F). The level of oxidatively damaged proteins in the cells exposed to TPM from THS2.2 aerosol for 1 week also seemed to be increased (especially for medium and high dose exposures); however, the effect was not statistically significant. Interestingly, in cells exposed to 3R4F TPM and the highest concentration of THS2.2 TPM (150 $\mu\text{g}/\text{mL}$) for 12 weeks (where no alterations in the cytosolic and mitochondrial ROS levels were observed), we also found increased levels of carbonylated proteins (Fig. 4F). This indicates that even with the lack of detectable changes in ROS levels, oxidative stress can be observed. This also confirms different cellular responses to the short vs chronic and the 3R4F TPM vs THS2.2 TPM exposures.

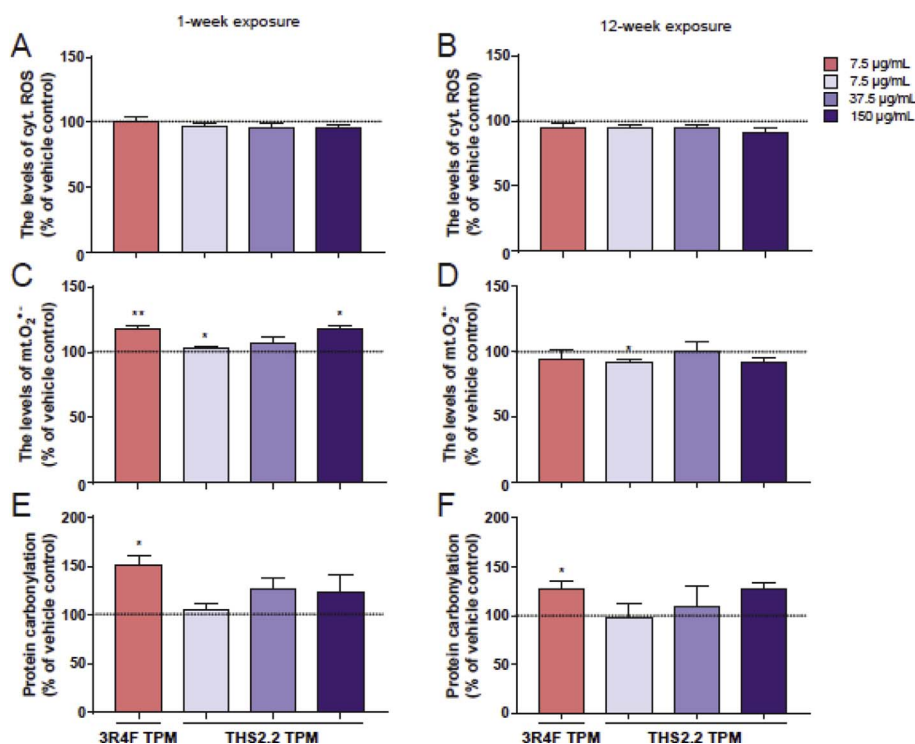


Fig. 4. Effects of total particulate matter (TPM) from 3R4F reference cigarette smoke (7.5 $\mu\text{g}/\text{mL}$) and THS2.2 aerosol (7.5, 37.5, and 150 $\mu\text{g}/\text{mL}$) on levels of (A, B) cytosolic reactive oxygen species (cyt.ROS), (C, D) mitochondrial superoxide (mt.O₂^{•-}), and (E, F) oxidatively damaged proteins. Levels of carbonylated proteins were calculated as a ratio to GAPDH. Data shown are means \pm SEM. *p < 0.05, **p < 0.01. cyt.ROS: n = 4; mt.O₂^{•-}: n = 4; protein carbonylation: n = 3–4 versus vehicle (DMSO)-exposed BEAS-2B cells.

3.6. The effect of short- and long-term exposure to TPM from 3R4F cigarette smoke and from THS2.2 aerosol on the expression levels of genes linked to the oxidative stress response in BEAS-2B cells

Cellular ROS levels depend on the balance between ROS production and detoxification by the antioxidant defense system. Taking into

account that the TPM exposures can affect the antioxidant defense system, we investigated the expression levels of genes linked to the oxidative stress response in TPM-exposed BEAS-2B cells. We focused on genes encoding antioxidant enzymes, genes involved in ROS metabolism as well as oxidative stress-responsive genes (Fig. 5). Interestingly, the gene expression patterns for the cells exposed to TPM from 3R4F

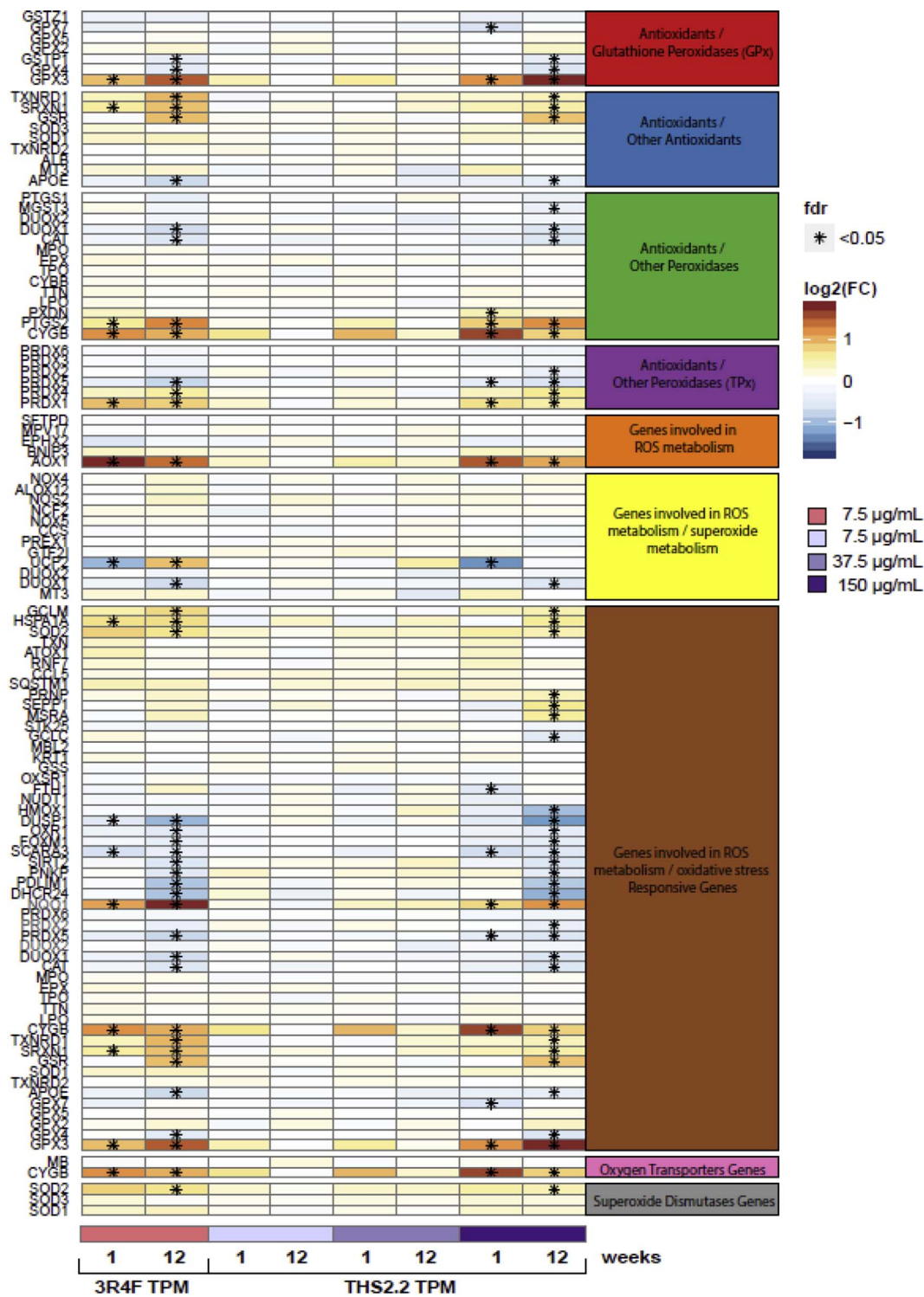


Fig. 5. Altered expression levels of genes linked to the oxidative stress response in BEAS-2B cells following exposure to total particulate matter (TPM) from 3R4F reference cigarette smoke or THS2.2 aerosol, compared with expression in unexposed controls, for 1 or 12 weeks. The heatmap depicts changes in gene expression for oxidative stress-related genes (gene symbols listed on the left) relative to those in corresponding non-exposed controls expressed as log2 fold-change (FC). Up- and down-regulation of gene expression levels is represented by orange and blue shades, respectively, with darker colors indicating greater absolute fold-changes. Statistically significant fold-changes are highlighted by * (adjusted p < 0.05). fdr, false discovery rate.

and the highest dose of TPM from THS2.2 (150 µg/mL) for 1 and 12 weeks were quite similar. The maximum changes in expression levels were observed in cells exposed for 12 weeks to both 3R4F CS and the highest concentration of TPM from THS2.2 aerosol (3R4F versus vehicle: 21 genes up- and 20 down-regulated; THS2.2 (150 µg/mL) versus vehicle: 22 genes up- and 25 down-regulated; FDR: < 0.05). Neither the low nor 5-fold higher concentrations of THS2.2 TPM (7.5 and 37.5 µg/mL) significantly changed expression of genes linked to oxidative stress in BEAS-2B cells over time. A number of up-regulated genes, including *PXDN*, *PRNP*, *SEPP1* and *MSRA* as well as down-regulated genes, including *GPX7*, *MGST3*, *PRDX2*, *GCLC*, and *FTH1* were exclusively affected by exposure to the highest concentration of THS2.2 TPM. Interestingly, *UCP2*, encoding mitochondrial uncoupling protein-2 which is involved in mitochondrial proton leakage and ROS control, was significantly down-regulated when BEAS-2B cells were exposed to TPM from 3R4F CS and the highest concentration of TPM from THS2.2 aerosol for 1 week. Twelve-week exposure to TPM from 3R4F CS also caused a strong up-regulation of *UCP2*, while gene expression levels returned to those in vehicle controls with the highest concentration of TPM from THS2.2 aerosol.

Moreover, we investigated the protein levels of the following antioxidant enzymes: two superoxide dismutases, SOD1 (present mostly in the cytosol and in the mitochondrial inner membrane space) and SOD2 (present in the mitochondrial matrix), as well as glutathione peroxidase isoform 1 (GPX1). As shown in Fig. 6C, 1-week exposure to 3R4F TPM had a strong effect on *GPX1* expression, decreasing the level of this antioxidant enzyme by around 60%. A similar effect of short 3R4F TPM exposure, albeit not statistically significant, was seen for SOD2 level. Exposure of BEAS-2B cells to the high dose of THS2.2 TPM (150 µg/mL) decreased the levels of all three antioxidant enzymes (Fig. 6A, 6B and 6C). These observations confirmed that the increased levels of mitochondrial superoxide and carbonylated proteins in cells exposed for 1 week can at least partially be caused by alterations in the antioxidant defense system, particularly with 3R4F TPM and high-dose THS2.2 TPM exposures. A different expression profile of oxidative stress-related genes was observed for 12-week TPM exposures. There was a small, but statistically significant increase in SOD1 in BEAS-2B cells exposed to the low and high dose (7.5 and 150 µg/mL) of TPM from THS2.2 aerosol

(Fig. 6D). 3R4F TPM exposure and exposure to the medium dose (37.5 µg/mL) of THS2.2 TPM also slightly increased SOD1 levels; however, this effect was not statistically significant. Interestingly, the level of SOD2 was decreased in BEAS-2B cells exposed to 3R4F TPM (Fig. 6E). On the other hand, the low and medium dose of TPM from THS2.2 aerosol increased SOD2 levels by about 20% ($p < 0.05$ only for low dose). 3R4F TPM exposure for 12 weeks also had the strongest effect on GPX1 levels which increased by about 20%, but which was also not statistically significant (Fig. 6F). Comparing the effect of 1- and 12-week exposures on the antioxidant defense system status, we observed different responses. However, regardless of this puzzling effect, oxidative stress as evidenced by increased levels of oxidatively damaged proteins was confirmed in BEAS-2B cells exposed to 3R4F TPM, and was independent of exposure duration. Alterations in the expression levels of genes for antioxidant enzymes additionally lends support to the presence of oxidative stress in cells exposed to the highest dose of TPM from THS2.2 aerosol for 12 weeks.

3.7. PCA analysis of effects of short- and long-term exposure to TPM from 3R4F cigarette smoke and THS2.2 aerosol on BEAS-2B cells

To compare the effects of TPM from 3R4F smoke and from THS2.2 aerosol after a 1- or 12-week exposure, principal component analysis (PCA) was performed. 15 parameters determined in this work were used for PCA analysis: Basal respiration, Proton leak, Maximal respiration, “respiration related to ATP production, Coupling efficiency, Spare Respiratory Capacity, the level of NDUFB8 - complex I, the level of SDHB - complex II, the level of UQCRC2 - complex III, the level of MTCO1 - complex IV, the level of ATP5A - ATP synthase, the level of cytosolic ROS, the level of mitochondrial superoxide, the level of carbonylated proteins and the level of ATP. PCA enabled a linear transformation of the six variables into a two-dimensional space, simultaneously retaining maximal information on individual variables. The new variables, PC1 and PC2, describe the similarities and differences between unexposed BEAS-2B cells, cells exposed to DMSO, and cells exposed to TPM from 3R4F CS and from THS2.2 aerosol (Fig. 7A and B). PCA showed noticeable differences between created profiles characteristic for 1 and 12 weeks exposure regimes. After 1 week of

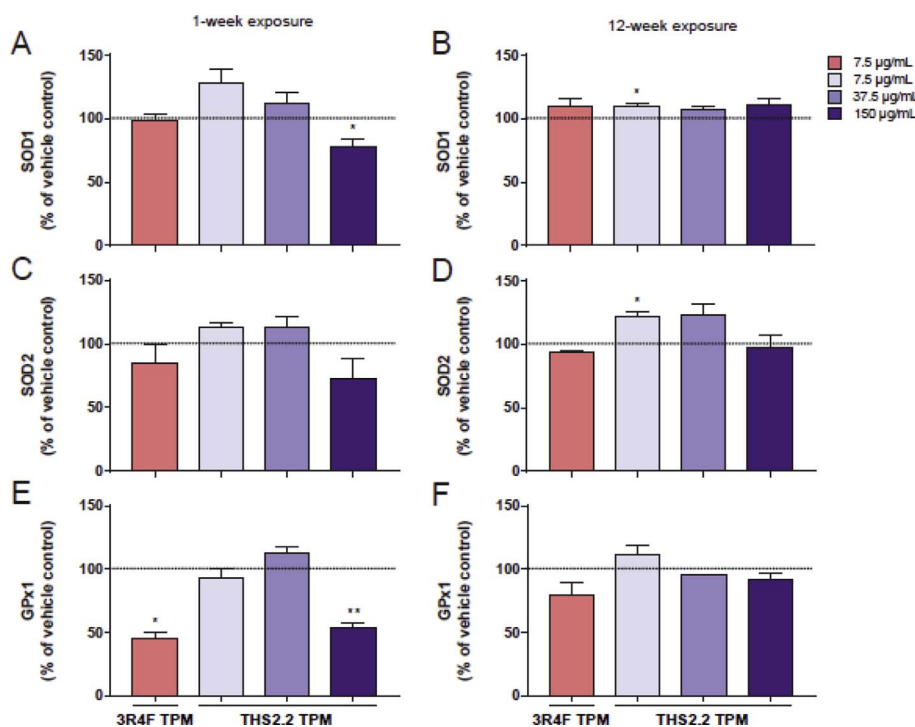


Fig. 6. Effects of total particulate matter (TPM) from 3R4F reference cigarette smoke (7.5 µg/mL) and THS2.2 aerosol (7.5, 37.5, and 150 µg/mL) on levels of the antioxidant enzymes SOD1, SOD2 and GPx1 in BEAS-2B cells. (A, B, C) Effects of a 1-week exposure. Antioxidant levels were calculated as a ratio to β -actin, and compared with levels in DMSO-exposed cells. Data shown are means \pm SEM. * $p < 0.05$, ** $p < 0.01$. SOD1: $n = 4$; SOD2: $n = 3$; GPx1: $n = 3$. (D, E, F) Effects of a 12-week exposure. Antioxidant levels were calculated as a ratio to β -actin, and compared with levels in DMSO-exposed cells. Data shown are means \pm SEM. * $p < 0.05$. SOD1: $n = 4$; SOD2: $n = 3$; GPx1: $n = 3$.

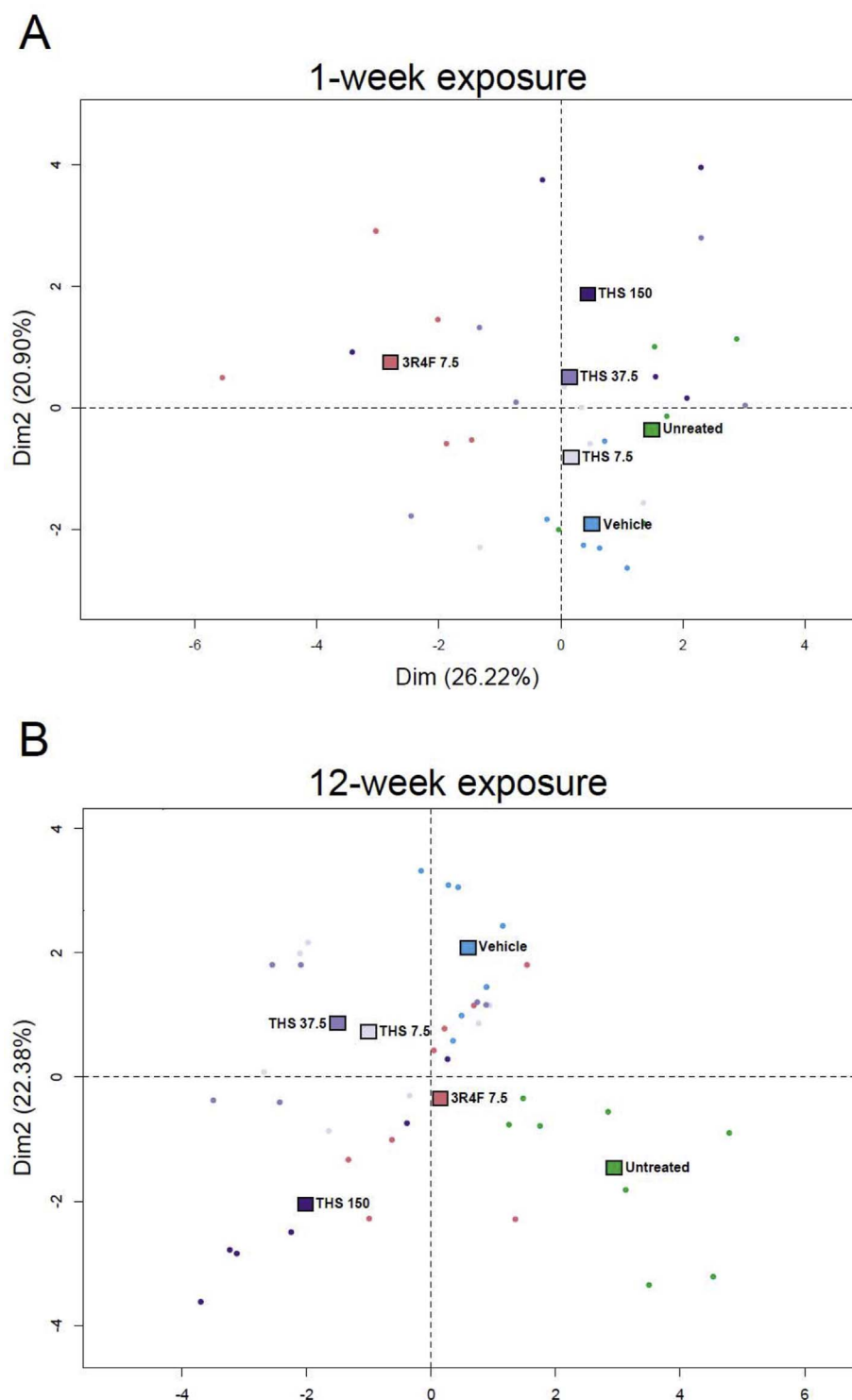


Fig. 7. Principal component analysis (PCA) showing the effects of DMSO, total particulate matter (TPM) from 3R4F reference cigarette smoke (7.5 µg/mL), and three concentrations of TPM from THS2.2 aerosol (7.5, 37.5 or 150 µg/mL) on the profile of investigated parameters in comparison with effects in unexposed BEAS-2B cells. 2D graph of variables PC1 and PC2 created based on 15 parameters (basal respiration, proton leak, maximal respiration, respiration related to ATP production, coupling efficiency, spare respiratory capacity, levels of representative subunits of the mitochondrial respiratory chain complexes [NDUFB8, SDHB, UQCRC2, MTCO1, ATP5A], levels of cytosolic reactive oxygen species, levels of mitochondrial superoxide [mt.O₂^{•-}], levels of carbonylated proteins, and levels of ATP) measured following (A) 1-week and (B) 12-week exposures.

exposure, the effects of TPM from 3R4F CS clearly differed from those of the other treatments (Fig. 7A). After 12 weeks of exposure, all exposed groups (exposures to TPM from 3R4F, DMSO, and TPM from THS2.2) differed from unexposed controls (Fig. 7B).

4. Discussion

Smoking enhances oxidative stress via several mechanisms, such as generation of ROS or alteration of antioxidant efficiency (Aoshiba and Nagai, 2003; Bialas et al., 2016; Bowler et al., 2004; Rahman and MacNee, 1999). Moreover, the harmful effects of smoke constituents on

mitochondria and the mitochondrial respiratory chain can cause impairment in ATP production and increased ROS production resulting from damaged respiratory chain complexes (Bialas et al., 2016; Cardellach et al., 2003; Miro et al., 1999; Zhang et al., 2017). In this study, we investigated the scale of mitochondrial respiratory chain dysfunction and manifestation of oxidative stress in BEAS-2B human bronchial epithelial cells following 1- and 12-week exposures to TPM from the aerosol of THS2.2 and from 3R4F reference CS.

There is a wealth of evidence concerning the influence of CS on cellular function; however, most *in vitro* studies using cultured cells have focused on the acute effects of CS exposure and thus employ

relatively short incubation times (usually up to 24 h) (Aug et al., 2014; Guan et al., 2013; van der Toorn et al., 2007; Zhang et al., 2017). Data on the effects of long-term exposures, which would resemble the *in vivo* situation more closely, are limited (Hoffmann et al., 2013; Veljkovic et al., 2011). Therefore, we were interested in highlighting the potential differences between short- and long-term exposures to TPM from 3R4F reference CS compared to aerosol from THS2.2.

The adverse effects of CS on mitochondrial respiratory chain function have been reported in isolated mitochondria (van der Toorn et al., 2007) as well as in cells and tissues of animals (Agarwal et al., 2014; Gvozdkajkova et al., 1999) and humans (Bouhours-Nouet et al., 2005; Cardellach et al., 2003; Miro et al., 1999). Similarly, in our study model (BEAS-2B cells), we observed decreased mitochondrial respiration (both basal and maximal rates) in cells exposed for 1 week to TPM from the 3R4F reference cigarette. This was accompanied by a decrease in the content of selected subunits of respiratory chain complexes I and II. This finding contradicts that of Hoffmann et al., who observed increased levels of the tested respiratory chain subunits in BEAS-2B cells exposed to CS extracts (Hoffmann et al., 2013). In that study, however, a much longer exposure duration of 6 months was applied. In addition, the dose-dependence of this effect was much stronger: above a certain CSE dose, the increase in the levels of respiratory chain proteins was smaller. Generally, there is discrepancy in the literature concerning the influence of CS exposure on the amount and activities of respiratory chain complexes: both increases (Agarwal et al., 2012; Hoffmann et al., 2013) and decreases (Cardellach et al., 2003; Miro et al., 1999) were reported, depending on the experimental model, investigated tissue, incubation time, and applied concentrations. Contrary to the 1-week exposure, the 12-week exposure of BEAS-2B cells to 3R4F TPM increased basal and maximal respiration rates as well as proton leak. This coincided with higher expression of *UCP2*, but the available data do not allow for a conclusion about the causal relationship between these two observations.

Among other aspects of mitochondrial function, we observed increased mitochondrial ROS levels in cells exposed for 1 week. Similar observations were also reported in human airway smooth muscle cells (Aravamudan et al., 2014) exposed to CSE for 24 h. The effect of antimycin A suggests that increased $\text{mt.O}_2^{\cdot-}$ levels was the result of elevated superoxide production by the respiratory chain, rather than of impaired ROS scavenging. Surprisingly, no changes in cytosolic ROS levels were detected in our study, contrary to findings in multiple studies using CS-exposed cultured cells, where elevation of ROS levels was observed (Lin et al., 2014; van der Toorn et al., 2009; Wylam et al., 2015). In these studies, however, shorter exposure times had been applied (up to 24 h) and typically higher concentrations, resulting in decreased cell viability. Despite the unaltered levels of cytosolic ROS in our study, we observed hallmarks of oxidative stress following both 1 and 12 weeks of exposure to TPM from CS, such as increased protein carbonylation and up- as well as down-regulated expression of oxidative stress response genes. Additionally, the levels of the antioxidant enzyme GPx1 decreased. In line with these findings, Zhang et al. reported multiple symptoms of oxidative stress and redox balance disruption after short exposure of BEAS-2B cells to CS, including a decreased ratio of reduced glutathione to oxidized glutathione and oxidative damage of lipids and DNA (Zhang et al., 2017).

Compared to 3R4F TPM, THS2.2 TPM needed to be applied at 20-fold higher concentration to cause a similar extent of oxidative stress and changes in cellular bioenergetics. 7.5 $\mu\text{g}/\text{mL}$ 3R4F TPM and 150 $\mu\text{g}/\text{mL}$ THS2.2 TPM exerted similar effects on mitochondrial superoxide levels, protein carbonylation and levels of GPx1. Gene expression analysis showed similar changes in expression patterns of oxidative stress response genes in cells exposed to 7.5 $\mu\text{g}/\text{mL}$ of TPM from reference CS and to 150 $\mu\text{g}/\text{mL}$ of TPM from THS2.2 aerosol. Both treatments decreased the levels of selected respiratory chain proteins, but a 1-week exposure to TPM from the reference cigarette induced a strong decrease in the levels of complex I subunit NDUF8, while TPM

from THS2.2 had a more pronounced effect on the levels of the complex IV subunit. The difference between the mechanisms of toxicity of TPM from 3R4F and THS2.2 was seen in their varied effects on respiration rates and glycolysis, where the reference cigarette caused stronger disturbances than even the highest concentration of TPM from THS2.2. These observations would suggest that different compounds in CS could be responsible for respiratory disturbances and for oxidative stress, and that these alterations may be caused, at least partially, by independent mechanisms.

The presence of oxidative stress was directly confirmed in BEAS-2B cells exposed to TPM from 3R4F CS for both 1 and 12 weeks by the increased levels of oxidatively damaged proteins. Moreover, based on the expression pattern of genes involved in ROS metabolism, the highest concentration of TPM from THS2.2 aerosol also caused oxidative stress even though the levels of cytosolic ROS and mitochondrial superoxide were unchanged. The greatest effect on expression levels of genes involved in ROS metabolism was observed in cells exposed for 12 weeks to TPM from 3R4F CS and the highest concentration of TPM from THS2.2 aerosol. Interestingly, when comparing results for the two exposure periods, the effects are usually stronger after shorter exposure. For some parameters, an opposite direction of changes are observed, as in the case of basal and maximal respiration rates, which decreased after 1-week exposure, but increased after 12-week exposure. Some of these differences may reflect adaptive mechanisms, allowing cells to survive under chronic stress conditions. It is, however, also known that long-term exposure of bronchial epithelial cells to CS results in persistent epigenetic changes characteristic of malignant transformation (Veljkovic et al., 2011), and we cannot exclude that some of the effects of long-term exposure are already reflecting this hallmark of cancer.

5. Conclusion

This study showed that alterations in mitochondrial respiratory chain function are accompanied by oxidative stress in BEAS-2B cells exposed to TPM from 3R4F CS and THS2.2 aerosol, and that the effects varied by exposure duration. A concentration of TPM from THS2.2 aerosol 20-fold higher than the concentration of TPM from 3R4F was required to disturb cellular function to a similar extent. This indicates that reducing levels of HPHCs by heating rather than combusting tobacco could reduce mitochondrial dysfunction and oxidative stress-related diseases associated with smoking combustible tobacco products.

Interestingly, the effect of TPM exposures on the mitochondrial respiratory chain is different between the two exposure durations. In contrast to the effects of short-term stress, a chronic exposure appears to result in cellular adaptation to the stressors. Future investigations should focus on elucidating the mechanism underlying this adaptation.

Conflict-of-interest statement

Alain Sewer, Stephanie Johne, Karsta Luettich, Manuel C Peitsch, Julia Hoeng, Marco van der Toorn are employees of and paid by Philip Morris International.

Philip Morris International was the sole source of funding and sponsor of this project.

Acknowledgments

This work was funded by Philip Morris International R&D.

The authors are grateful to V. Biernat for specialist technical assistance.

Transparency document

Transparency document related to this article can be found online at <http://dx.doi.org/10.1016/j.fct.2018.02.013>.

Appendix A. Supplementary data

Supplementary data related to this article can be found at <http://dx.doi.org/10.1016/j.fct.2018.02.013>.

References

- Agarwal, A.R., Zhao, L., Sancheti, H., Sundar, I.K., Rahman, I., Cadenas, E., 2012. Short-term cigarette smoke exposure induces reversible changes in energy metabolism and cellular redox status independent of inflammatory responses in mouse lungs. *American journal of physiology. Lung cellular and molecular physiology* 303, L889–L898.
- Agarwal, A.R., Yin, F., Cadenas, E., 2014. Short-term cigarette smoke exposure leads to metabolic alterations in lung alveolar cells. *Am. J. Respir. Cell Mol. Biol.* 51, 284–293.
- Anbarasi, K., Vani, G., Devi, C.S., 2005. Protective effect of bacoside A on cigarette smoking-induced brain mitochondrial dysfunction in rats. *J. Environ. Pathol. Toxicol. Oncol.* 24, 225–234.
- Ashiba, K., Nagai, A., 2003. Oxidative stress, cell death, and other damage to alveolar epithelial cells induced by cigarette smoke. *Tob. Induc. Dis.* 1, 219–226.
- Aravamudan, B., Kiel, A., Freeman, M., Delmotte, P., Thompson, M., Vassallo, R., Sieck, G.C., Pabelick, C.M., Prakash, Y.S., 2014. Cigarette smoke-induced mitochondrial fragmentation and dysfunction in human airway smooth muscle. *American journal of physiology. Lung cellular and molecular physiology* 306, L840–L854.
- Aug, A., Altraja, A., Altraja, S., Laaniste, L., Mahlapuu, R., Soomets, U., Kilk, K., 2014. Alterations of bronchial epithelial metabolome by cigarette smoke are reversible by an antioxidant, O-methyl-L-tyrosinyl-gamma-L-glutamyl-L-cysteinylglycine. *Am. J. Respir. Cell Mol. Biol.* 51, 586–594.
- Baker, R.R., 1974. Temperature distribution inside a burning cigarette. *Nature* 247, 405–406.
- Barsanti, K.C., Luo, W., Isabelle, L.M., Pankow, J.F., Peyton, D.H., 2007. Tobacco smoke particulate matter chemistry by NMR. *Magn. Reson. Chem.* 45, 167–170.
- Benjamini, Y., Hochberg, Y., 1995. Controlling the false discovery rate: a practical and powerful approach to multiple testing. *J. Roy. Stat. Soc. B* 289–300.
- Bialas, A.J., Sitarek, P., Milkowska-Dymanowska, J., Piotrowski, W.J., Gorski, P., 2016. The role of mitochondria and oxidative/antioxidative imbalance in pathobiology of chronic obstructive pulmonary disease. *Oxid Med Cell Longev* 2016 7808576.
- Bouhours-Nouet, N., May-Panloup, P., Coutant, R., de Casson, F.B., Descamps, P., Douay, O., Reynier, P., Ritz, P., Malhiery, Y., Simard, G., 2005. Maternal smoking is associated with mitochondrial DNA depletion and respiratory chain complex III deficiency in placenta. *Am. J. Physiol. Endocrinol. Metab.* 288, E171–E177.
- Bowler, R.P., Barnes, P.J., Crapo, J.D., 2004. The role of oxidative stress in chronic obstructive pulmonary disease. *COPD* 1, 255–277.
- Bradford, M.M., 1976. A rapid and sensitive method for the quantitation of microgram quantities of protein utilizing the principle of protein-dye binding. *Anal. Biochem.* 72, 248–254.
- Cardellach, F., Alonso, J.R., Lopez, S., Casademont, J., Miro, O., 2003. Effect of smoking cessation on mitochondrial respiratory chain function. *J. Toxicol. Clin. Toxicol.* 41, 223–228.
- Durham, A.L., Adcock, I.M., 2015. The relationship between COPD and lung cancer. *Lung Canc.* 90, 121–127.
- Guan, S.P., Tee, W., Ng, D.S., Chan, T.K., Peh, H.Y., Ho, W.E., Cheng, C., Mak, J.C., Wong, W.S., 2013. Andrographolide protects against cigarette smoke-induced oxidative lung injury via augmentation of Nrf2 activity. *Br. J. Pharmacol.* 168, 1707–1718.
- Gvozdkajova, A., Simko, F., Kucharska, J., Braunova, Z., Psenek, P., Kyselovic, J., 1999. Captopril increased mitochondrial coenzyme Q10 level, improved respiratory chain function and energy production in the left ventricle in rabbits with smoke mitochondrial cardiomyopathy. *Biofactors* 10, 61–65.
- Health Canada, 1999. Health Canada Test Method T-115, Determination of “Tar” and Nicotine in Sidestream Tobacco Smoke.
- Hoffmann, R.F., Zarrintan, S., Brandenburg, S.M., Kol, A., de Bruin, H.G., Jafari, S., Dijk, F., Kalicharan, D., Kelders, M., Gosker, H.R., Ten Hacken, N.H., van der Want, J.J., van Oosterhout, A.J., Heijink, I.H., 2013. Prolonged cigarette smoke exposure alters mitochondrial structure and function in airway epithelial cells. *Respir. Res.* 14, 97.
- CDC, 2010. Tobacco Smoke Causes Disease: The Biology and Behavioral Basis for Smoking-attributable Disease: a Report of the Surgeon General, Atlanta (GA).
- International Organization for Standardization, 2010. ISO 3402: 1999–Tobacco and Tobacco Products – Atmosphere for Conditioning and Testing, fourth ed. .
- Lebiedzinska, M., Karkucinska-Wieckowska, A., Wojtala, A., Suski, J.M., Szabadkai, G., Wilczynski, G., Wlodarczyk, J., Diogo, C.V., Oliveira, P.J., Tauber, J., Jezek, P., Pronicki, M., Duszynski, J., Pinton, P., Wieckowski, M.R., 2013. Disrupted ATP synthase activity and mitochondrial hyperpolarisation-dependent oxidative stress is associated with p66Shc phosphorylation in fibroblasts of NARP patients. *Int. J. Biochem. Cell Biol.* 45, 141–150.
- Liberti, M.V., Locasale, J.W., 2016. The Warburg effect: how does it benefit cancer cells? *Trends Biochem. Sci.* 41, 211–218.
- Lin, X.X., Yang, X.F., Jiang, J.X., Zhang, S.J., Guan, Y., Liu, Y.N., Sun, Y.H., Xie, Q.M., 2014. Cigarette smoke extract-induced BEAS-2B cell apoptosis and anti-oxidative Nrf-2 up-regulation are mediated by ROS-stimulated p38 activation. *Toxicol. Mech. Meth.* 24, 575–583.
- Miro, O., Alonso, J.R., Jarreta, D., Casademont, J., Urbano-Marquez, A., Cardellach, F., 1999. Smoking disturbs mitochondrial respiratory chain function and enhances lipid peroxidation on human circulating lymphocytes. *Carcinogenesis* 20, 1331–1336.
- Patskan, G., Reininghaus, W., 2003. Toxicological evaluation of an electrically heated cigarette. Part 1: overview of technical concepts and summary of findings. *J. Appl. Toxicol.* 23, 323–328.
- Rahman, I., MacNee, W., 1996. Role of oxidants/antioxidants in smoking-induced lung diseases. *Free Radical Biol. Med.* 21, 669–681.
- Rahman, I., MacNee, W., 1999. Lung glutathione and oxidative stress: implications in cigarette smoke-induced airway disease. *Am. J. Physiol.* 277, L1067–L1088.
- Rodgman, A., Perfetti, T., 2013. The Chemical Components of Tobacco and Tobacco Smoke, second ed. CRC Press, pp. 2238.
- Smith, M.R., Clark, B., Luedicke, F., Schaller, J.P., Vanscheuwijck, P., Hoeng, J., Peitsch, M.C., 2016. Evaluation of the tobacco heating system 2.2. Part 1: description of the system and the scientific assessment program. *Regul. Toxicol. Pharmacol.* 81 (Suppl. 2), S17–S26.
- Smyth, G.K., 2005. Limma: Linear Models for Microarray Data. *Bioinformatics and Computational Biology Solutions Using R and Bioconductor*. Springer, pp. 397–420.
- van der Toorn, M., Slebos, D.J., de Bruin, H.G., Leuvenink, H.G., Bakker, S.J., Gans, R.O., Koeter, G.H., van Oosterhout, A.J., Kauffman, H.F., 2007. Cigarette smoke-induced blockade of the mitochondrial respiratory chain switches lung epithelial cell apoptosis into necrosis. *American journal of physiology. Lung cellular and molecular physiology* 292, L1211–L1218.
- van der Toorn, M., Rezayat, D., Kauffman, H.F., Bakker, S.J., Gans, R.O., Koeter, G.H., Choi, A.M., van Oosterhout, A.J., Slebos, D.J., 2009. Lipid-soluble components in cigarette smoke induce mitochondrial production of reactive oxygen species in lung epithelial cells. *American journal of physiology. Lung cellular and molecular physiology* 297, L109–L114.
- van der Toorn, M., Sewer, A., Marescotti, D., John, S., Baumer, K., Bornand, D., Dulize, R., Merg, C., Corciulo, M., Scotti, E., Pak, C., Leroy, P., Guedj, E., Ivanov, N., Martin, F., Peitsch, M., Hoeng, J., Luettich, K., 2018. The biological effects of long-term exposure of human bronchial epithelial cells to total particulate matter from a candidate modified-risk tobacco product. *Toxicol. Vitro* (in press).
- Veljkovic, E., Jiricny, J., Menigatti, M., Rehrauer, H., Han, W., 2011. Chronic exposure to cigarette smoke condensate in vitro induces epithelial to mesenchymal transition-like changes in human bronchial epithelial cells, BEAS-2B. *Toxicol. Vitro* 25, 446–453.
- Wojewoda, M., Duszynski, J., Szczepanowska, J., 2010. Antioxidant defence systems and generation of reactive oxygen species in osteosarcoma cells with defective mitochondria: effect of selenium. *Biochim. Biophys. Acta* 1797, 890–896.
- Wojewoda, M., Duszynski, J., Szczepanowska, J., 2011. NARP mutation and mtDNA depletion trigger mitochondrial biogenesis which can be modulated by selenium supplementation. *Int. J. Biochem. Cell Biol.* 43, 1178–1186.
- Wong, E.T., Kogel, U., Veljkovic, E., Martin, F., Xiang, Y., Boue, S., Vuillaume, G., Leroy, P., Guedj, E., Rodrigo, G., Ivanov, N.V., Hoeng, J., Peitsch, M.C., Vanscheuwijck, P., 2016. Evaluation of the Tobacco Heating System 2.2. Part 4: 90-day OECD 413 rat inhalation study with systems toxicology endpoints demonstrates reduced exposure effects compared with cigarette smoke. *Regul. Toxicol. Pharmacol.* 81 (Suppl. 2), S59–S81.
- Wylam, M.E., Sathish, V., VanOosten, S.K., Freeman, M., Burkholder, D., Thompson, M.A., Pabelick, C.M., Prakash, Y.S., 2015. Mechanisms of cigarette smoke effects on human airway smooth muscle. *PLoS One* 10 e0128778.
- Zhang, S., Li, X., Xie, F., Liu, K., Liu, H., Xie, J., 2017. Evaluation of whole cigarette smoke induced oxidative stress in A549 and BEAS-2B cells. *Environ. Toxicol. Pharmacol.* 54, 40–47.